Journal of Applied Polymer Science

PMMA Composites of Single-Walled Carbon Nanotubes-*graft*-PMMA

Abhijit Paul,[1] Brian P. Grady,[2] Warren T. Ford[1]*

[1]Department of Chemistry, Oklahoma State University, Stillwater, Oklahoma 74078

[2]Carbon Nanotube Technology Center (CaNTeC) and School of Chemical, Biological, and Materials Engineering, University of Oklahoma, Norman, Oklahoma 73019

*Present address: Department of Chemistry, Portland State University, Portland, Oregon, 97207

Correspondence to: W. T. Ford (E-mail: warren.ford@okstate.edu)

ABSTRACT: To facilitate the dispersion of single-walled carbon nanotubes (SWCNT) into poly(methyl methacrylate) (PMMA), SWCNT were functionalized with a RAFT chain transfer agent, and PMMA was grafted from the SWCNT by reversible addition–fragmentation transfer (RAFT) polymerization to give SWCNT-*g*-PMMA containing 6 wt % PMMA. SWCNT-*g*-PMMA in the form of small bundles was dispersed into PMMA matrices. The SWCNT-*g*-PMMA filler increased the glass transition temperature (T_g) of the composite when the matrix molecular weight M_n was less than the graft molecular weight, but not when the matrix M_n was equal to or greater than the graft M_n. The threshold of electrical conductivity of the composites as a function of weight percent SWCNT increased from 0.2% when matrix M_n was less than graft M_n to about 1% when matrix M_n was greater than graft M_n. Dynamic mechanical analyses of the composites having graft M_n less than or equal to matrix M_n showed broader rubbery plateaus with increased SWCNT content but no significant differences between samples with different grafted PMMAs. The results indicate that lower M_n matrix wets the SWCNT-*g*-PMMA whereas higher M_n matrix does not wet the SWCNT-*g*-PMMA. © 2013 Wiley Periodicals, Inc. J. Appl. Polym. Sci. **2014**, *131*, 39884.

KEYWORDS: composites; grafting; functionalization of polymers; nanotubes; graphene and fullerenes

Received 28 May 2013; accepted 22 August 2013

DOI: 10.1002/app.39884

INTRODUCTION

Dispersing carbon nanotubes into a polymer promises to increase the mechanical strength and the electrical and thermal conductivity of the polymer.[1–4] However, in practice, carbon nanotube filler has produced only minor improvements in the mechanical properties of most polymers.[1] The smaller the diameter of carbon nanotubes, the more difficult the tubes are to disperse in solvents or polymers. Unfunctionalized single-walled carbon nanotubes (SWCNT) generally disperse into solvents in the form of individual tubes or small bundles stabilized by adsorption of surfactants or polymers.[1] Alternatively the SWCNT can be functionalized covalently to decrease the strong intertube van der Waals attractions and increase the surface energy of the tube which both aid in dispersion.[1] While added surfactants and polymers are generally detrimental to the properties of a composite, functionalization of the nanotube surface with a polymer chemically identical with the matrix avoids additives and should aid dispersion.

Polymer mixing, however, is not that simple. Theory and experiments on polymer brushes grafted on planar surfaces[5–10] and on curved surfaces[11–19] in a chemically identical matrix show that usually the matrix polymer wets the polymer brush if the molecular weight of the matrix is less than the molecular weight of the graft, but not if the molecular weight of the matrix polymer is greater than that of the graft. This phenomenon is known as "autophobic dewetting," and is due to a decrease in entropy when the higher molecular weight matrix is mixed with the lower molecular weight graft chains. The conformations of polymer chains anchored to a surface depend on the curvature of the surface relative to the dimensions of the polymer. At the same grafting density (in chains nm^{-2}), polymer chains anchored to a curved surface of a sphere or a cylinder of radius less than the radius of gyration of the polymer become less densely packed with increasing distance from the surface than polymer chains anchored to a flat surface.[12–14,16–19] Thus autophobic dewetting becomes less probable as the radius of curvature of the surface decreases; for example, by comparison of a planar silica surface, where grafted polymer chains extend in one dimension, to the surface of a silica nanoparticle, where grafted polymer chains extend in three dimensions.

Additional Supporting Information may be found in the online version of this article.

Autophobic dewetting also becomes less probable as the density of grafted chains decreases.[9] In this article, we report PMMA grafted at low density to the surface of bundles of SWCNT, in which the grafted polymer chains extend in two dimensions, as a function of the relative molecular weights of the grafted and the matrix PMMA chains. Thermal analyses of the SWCNT-*g*-PMMA/PMMA composites are consistent with autophobic dewetting even at low graft density when the matrix chains are longer than the chains grafted to the bundles of SWCNT. Previously we reported that T_g of SWCNT/polystyrene (PS) and of low graft density SWCNT-*g*-PS/PS composites increases with increasing SWCNT content using broad polydispersity PS rather than the narrow polydispersity PMMA of this investigation.[20–22]

EXPERIMENTAL

Materials

Methyl methacrylate (99.0%, Aldrich) was purified by passing though activated basic alumina. Thionyl chloride (Aldrich, 99+%), tetrahydrofuran (THF, HPLC grade, Aldrich), triethylamine (TEA, Aldrich, ≥99.5%), 4-(dimethylamino)pyridine (DMAP, Aldrich, ≥99.0%), *N,N′*-dicyclohexylcarbodiimide (DCC, Aldrich, ≥99.0%), and $CDCl_3$ (Aldrich, 99.8 atom% D) were used as received. Ethylene glycol (EG, Acros, 97%) was distilled at 1 atm pressure. 1-Methyl-2-pyrrolidinone (NMP, anhydrous, 99.5%), *N,N*-dimethylformamide (DMF), and 1,2-dichlorobenzene (DCB) were used as received from Aldrich or Acros Chemicals. Azobisisobutyronitrile (AIBN, Aldrich, 98%) was recrystallized from methanol. The RAFT chain transfer agent (CTA) 4-cyano-4-(dodecylsulfanylthiocarbonyl)sulfanylpentanoic acid (min. 97%) was purchased from Strem Chemicals. SWCNT (CoMoCat, Lot # SG76-000-020) was provided by Southwest Nanotechnologies (Norman, OK). The manufacturer reported diameter 0.93 ± 0.27 nm, aspect ratio 1000, >90 wt % carbon, ~8–10% Mo oxide, and >50% tubes of (7,6) chirality. Water was triply deionized.

Instruments and Measurements

The molar masses of PMMA were measured by size exclusion chromatography (SEC) using THF as eluent at 1 mL min^{-1} and 40°C with differential refractive index detection and a single Polymer Laboratories column (PL gel 5 μm mixed B, 300 mm length × 7.5 mm internal diameter). PMMA standards in the range 600,000–800 g mol^{-1} were used for calibration. A 35 μL sample solution (5 mg mL^{-1} in THF) was injected. Thermogravimetric analyses (TGA) were carried out in a nitrogen atmosphere at a heating rate of 10°C min^{-1} with a Mettler Toledo TGA/DSC/1, STAR^e System instrument. The wt % of PMMA grafted onto the nanotube surface was calculated from the TGA plots at 600°C as 100(wt % RAFT agent grafted SWCNT – wt % SWCNT-*g*-PMMA)/(wt % RAFT agent grafted SWCNT). The amounts of RAFT agents attached to the SWCNT surface were measured by elemental analyses for S at Atlantic Microlab, GA. SWCNT samples were dispersed in solvents using a Fisher FS-30 160W 3QT ultrasonic cleaner or a Microson XL-2000 22 KHz ultrasonic cell disruptor. The dispersions were filtered using a vacuum glass filtration cell and Fluoropore 0.2 μm PTFE filters from Millipore. SWCNT-*g*-PMMA were precipitated using a DAMON IEC EXD centrifuge. Raman spectroscopy was carried out on solid samples using a Coherent He-Ne laser at 633 nm at 20 mW with a scan time of 10 s. Scanning transmission electron microscopy (STEM) images were obtained with a JEOL JEM-2100 instrument at 200 kV accelerating voltage. Samples were prepared by diluting 1 mL (0.45 mg of SWCNT) of SWCNT-*g*-PMMA dispersion in NMP with 20 mL of THF, centrifuging at 8400 × *g* for 15 min, and redispersing the solids in THF four times. The solid SWCNT-*g*-PMMA was dispersed in 2 mL of THF and bath sonicated for 5 min. Two drops of THF dispersion were deposited onto an ultrathin carbon film/holey carbon 400 mesh copper grid (Ted Pella). UV/vis/NIR spectra were obtained using a Varian 5000 spectrophotometer. Stock dispersions of 0.015 g SWCNT L^{-1} in NMP were centrifuged for 30 min at 540 × *g* and allowed to stand for 3 h. The dark supernatant solution was used to obtain the spectra. Differential scanning calorimetry (DSC) data of SWCNT-*g*-PMMA/PMMA nanocomposites were recorded at the scan rate of 10°C min^{-1} after quick cooling from elevated temperature.[20] Electrical conductivities were tested by a two-point probe method with a specially constructed resistivity chamber, calibrated by a Keithley 610C Electrometer. Dynamic mechanical analysis (DMA) measurements of the storage and loss moduli of 30 × 5 × 0.5 mm^3 SWCNT-*g*-PMMA/PMMA composite samples were made with a Rheometric Scientific RSA II instrument. All experiments were performed with a 1 Hz frequency, 0.05% strain, and static force tracking dynamic force. The temperature was ramped between −90 and ~250°C. The samples were equilibrated for 1 min at a given temperature before measurement with a 4 K interval between data points. T_g was determined from the temperature corresponding to the peak in tan δ.

SWCNT–COOH[21]

A 500 mL glass bottle was charged with 0.34 g of SWCNT and 300 mL of DMF. The mixture was bath sonicated at 25°C for 1 h followed by 12 h stirring. Then tubes were vacuum filtered through a 0.2 μm PTFE membrane, and washed with water and small amounts of methanol. Immediately, the tubes were dispersed in 680 mL of 8 M HNO_3, stirred for 10 min, and bath sonicated for 2 h at 55–60°C. The mixture was cooled to 25°C, diluted with 200 mL of water, and vacuum filtered. The tubes were washed with water until the pH was >6. The solid collected on the filter was washed with 30 mL of methanol, and a small amount of DCB and kept wet.

SWCNT–OH[22]

All of the SWCNT–COOH were dispersed in 300 mL of $SOCl_2$ in a three necked 500 mL round bottomed flask, bath sonicated, and stirred magnetically for 5 min. DCB (25 mL) was added and heated at 70°C for 30 h under nitrogen, 50 mL more of DCB was added to the flask, and the $SOCl_2$ was distilled off at 1 atm. The SWCNT–COCl dispersion was added to 300 mL of THF and vacuum filtered. The solid on the filter was washed with a small amount of NMP and dispersed into NMP at concentration ~0.5 g L^{-1}. The mixture was stirred for 15 min, bath sonicated for 1 h, and stirred for 24 h.

A 1000 mL round bottomed flask was charged with all of the SWCNT–COCl/NMP dispersion. The mixture was tip sonicated for 15 min at 15 W output. DMAP (0.13 g, 1.1 mmol), 6.8 g of ethylene glycol (6.1 mmol), and 10 mL of triethylamine were added to the mixture and stirred for 96 h under nitrogen in the

dark. The mixture was vacuum filtered and washed with THF, methanol, and dichloromethane. The solid SWCNT–OH was dispersed in dichloromethane (dried over 3 Å molecular sieves) overnight.

SWCNT-RAFT

The RAFT agent was immobilized on the SWCNT by a method described elsewhere for 4-cyano-4-(dodecylsulfanylthiocarbonyl)sulfanylpentanoic acid.[23] A 1000 mL round bottomed flask was charged with all of the SWCNT–OH/dichloromethane dispersion. The mixture was bath sonicated for 30 min with magnetic stirring under nitrogen. DCC (1.1 g, 5.4 mmol), DMAP (0.13 g, 1.1 mmol), CTA (1.4 g, 3.5 mmol), and 15 mL of dry dichloromethane were stirred for 10 min under nitrogen. The solution was added to the SWCNT–OH/dichloromethane dispersion, and mixture was stirred at 25°C for 24 h in the dark. The SWCNT-CTA were filtered and washed with an excess of the amount of dichloromethane needed to dissolve the dicyclohexylurea, methanol, and NMP. The SWCNT-CTA were dispersed in NMP at ~0.5 g L^{-1}, bath sonicated for 15 min, and stirred overnight under nitrogen.

SWCNT-g-PMMA

The SWCNT-CTA dispersion was divided into three equal portions. Each portion was used to graft PMMA as follows. A 500 mL round bottomed flask was charged with 206 mL of SWCNT-RAFT/NMP dispersion (~0.5 g L^{-1}), MMA (5 g, 50 mmol) and 0.5 mg (0.003 mmol) of AIBN (0.1 mL of a stock solution of 50 mg AIBN in 10 mL of MMA). Four freeze-pump-thaw cycles were applied to remove dissolved oxygen. The solution was bath sonicated for 15 min and immersed in an oil bath at 90°C with constant stirring. After 96 h the mixture was cooled, diluted with 200 mL of THF, bath sonicated for 2 min, stirred for 15 min, and centrifuged at 540 × *g* for 30 min, and the supernatant liquid containing ungrafted PMMA was decanted. The cycle of centrifugation and redispersion in THF was repeated three times to obtain SWCNT-*g*-PMMA free of unbound PMMA. The mixture was vacuum filtered and washed with THF until the filtrate showed no cloudiness in excess methanol. The solid was washed with a small amount of NMP and dispersed in 210 mL of NMP, bath sonicated for 15 min and stirred for 24 h.

Cleavage of Grafted PMMA from SWCNT

The grafted PMMA was cleaved from the SWCNT surface by a method described elsewhere.[22] A 100 mL round bottomed flask was charged with 20 mg of SWCNT-*g*-PMMA dispersed in 5 mL of $CDCl_3$, 20 mL of DCB, 7 mL of methanol, and 0.5 mL of concentrated sulfuric acid. A water condenser was attached to the flask, and the mixture was stirred at 65°C for 7 days. After cooling, the mixture was sonicated for 2 min with 15 mL of $CHCl_3$, vacuum filtered, and washed twice with 10 mL of chloroform slowly with stirring to remove traces of PMMA. The filtrate was washed three times with 10 mL of DI water to remove H_2SO_4. The organic phase which contained cleaved PMMA was separated, and the organic solvent was removed under the vacuum. The residual PMMA was dispersed in 15 mL of THF which was evaporated to 2 mL for SEC analysis. After the SEC analysis the THF was evaporated to dryness, and 0.5 mL of $CDCl_3$ was added for ^{1}H-NMR analysis.

Ungrafted PMMA

A mixture of a stock solution of MMA (24.1 g, 241 mmol), AIBN (0.01 g, 0.06 mmol), and NMP (11.9 mL) was added to a 100 mL Schlenk flask containing a weighed amount of the RAFT agent. The reaction contents were degassed by four freeze-pump-thaw cycles, and the flask was heated in an oil bath at 90°C for 6 h. After cooling the viscous PMMA was dissolved in 10 mL of dichloromethane and precipitated into a 10-fold excess of methanol. The solid PMMA-RAFT was vacuum dried at 100°C for 48 h. The yield of PMMA was determined gravimetrically.

SWCNT-g-PMMA/PMMA Composites

SWCNT-*g*-PMMA was dispersed in NMP by bath sonication for 15 min followed by 24 h stirring at 25°C. The concentration of SWCNT in an NMP dispersion was measured by filtering 10 mL of the dispersion on a pre-weighed PTFE filter, washing with THF, and vacuum drying at 100°C for 24 h. The weight of solid on the filter and the wt % of grafted PMMA on SWCNT obtained from the TGA analysis were used to calculate the amount of SWCNT dispersed in the NMP. The SWCNT concentrations in the SWCNT-*g*-PMMA/NMP dispersions were 0.42–0.47 g L^{-1}. A dispersion of SWCNT-*g*-PMMA in NMP and a solution of matrix PMMA in THF (1.5 g in 20 mL) were mixed to yield the desired wt % of SWCNT in the final composite. The mixture was stirred mechanically for 15 min, bath sonicated at room temperature for 15 min, and precipitated dropwise into a large excess of 10 wt % aqueous solution of $CaCl_2$ with vigorous mechanical stirring. The composite was filtered, washed with water until the filtrate showed no white precipitate in 0.05*M* $AgNO_3$(aq) solution, washed with a small amount of methanol, and dried under vacuum at 130°C for 24 h. Composite samples having dimensions 2.5 × 2.5 × 0.02 $inch^3$ pressed in a mold at 1600 psi and 180°C for 1 min. Films were cooled to room temperature under the same pressure.

RESULTS

PMMA Grafting from SWCNT

There are several general methods for preparation of SWCNT and numerous types of SWCNT available. We used CoMoCat tubes from Southwest Nanotechnologies, which had average diameter 0.93 nm and contained more than 50% semiconducting tubes of (7,6) chirality. To improve their dispersability in solvent for functionalization, tubes were treated with nitric acid by a method that introduces small amounts of carboxylic acid groups and does not destroy any of the tubes.[21] The residual metal oxide content from the cobalt–molybdenum on silica catalyst after nitric acid treatment of this type of SWCNT is 3%.[21] All synthetic procedures were carried out with wet (not dried) modified SWCNT to facilitate dispersion.[24,25]

Carboxylic acid groups on the SWCNT were converted to trithiocarbonate RAFT agent by the method of Scheme 1. The amount of RAFT agent on the SWCNT was calculated to be 1.1 RAFT agent per 1000 nanotube C atoms from the sulfur content and an assumed 95 wt % of SWCNT carbon atoms in the

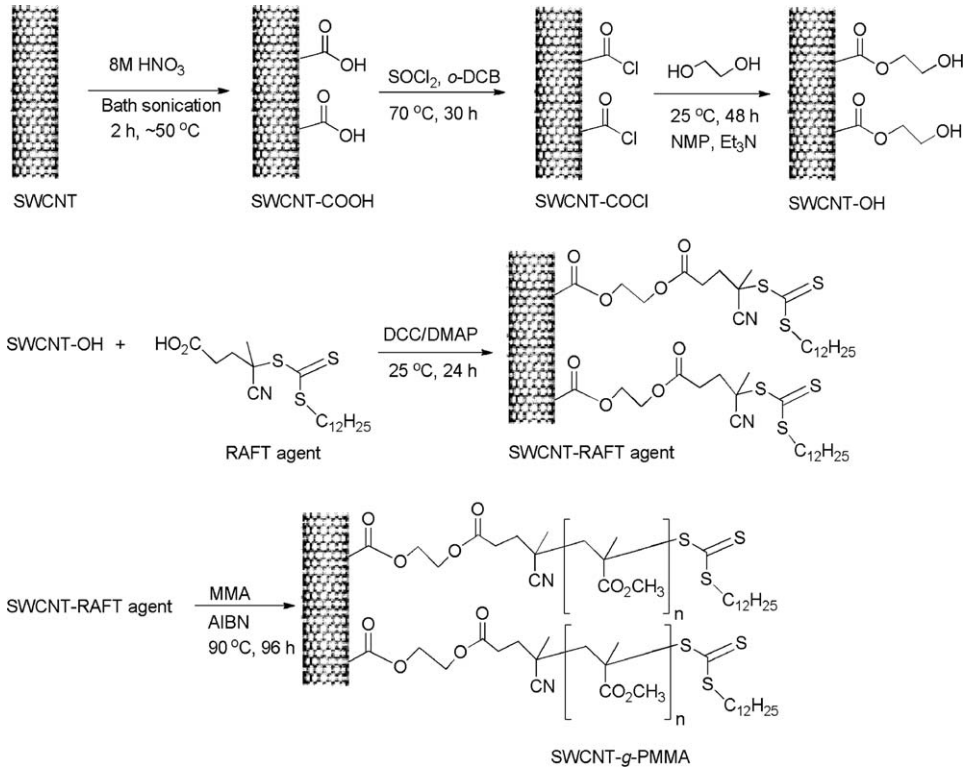

Scheme 1. Grafting of PMMA from SWCNT by RAFT polymerization.

material. The sulfur content was measured by elemental analysis of two different samples to average 0.85 wt %. A ^{1}H NMR spectrum of the SWCNT-RAFT material in $CDCl_3$ (Supporting Information Figure S1) had distinct peaks for all of the protons of the RAFT structure like the spectrum of the starting RAFT agent but with some changes in chemical shifts, which indicates a significant degree of functionalization with the RAFT structure.

Three different samples of PMMA grafted from SWCNT were prepared by RAFT polymerization under the same conditions. Simultaneously some ungrafted free PMMA was formed. Free PMMA and SWCNT-*g*-PMMA were separated by filtration and thorough washing of the retained SWCNT material with THF. Part of each SWCNT-*g*-PMMA sample was treated with strong acid to cleave the PMMA. PMMA samples both from the filtrates and from the SWCNT-*g*-PMMA were analyzed by SEC. The results are in Table I. The three PMMA samples recovered from the filtrates had the same molecular weights within experimental error and polydispersities of 1.23–1.32. The three PMMA samples recovered by cleavage from the SWCNT-*g*-PMMA had higher and more varied molecular weights, and polydispersities of 1.14–1.39. Cleaved PMMA had a ^{1}H NMR spectrum like that of ordinary PMMA from radical polymerization. All of the data show that all PMMA samples were produced by controlled polymerization, and that the soluble polymers were not identical with the grafted polymers.

Table I. SEC Analyses of Grafted and Free PMMA

Grafted PMMA[a]		Free PMMA[b]	
M_n (g mol^{-1})	M_w/M_n	M_n (g mol^{-1})	M_w/M_n
22,600	1.39	19,100	1.23
26,000	1.31	18,200	1.24
35,700	1.14	18,700	1.32

[a] PMMA recovered after cleavage from SWCNT.
[b] PMMA recovered from the filtrate of the grafting reaction mixture. Molecular weights are the average of two analyses of one sample.

Thermogravimetric analyses (TGA) of commercial SWCNT, nitric acid treated SWCNT, SWCNT-RAFT, and three different SWCNT-*g*-PMMA samples are shown in Figure 1 with weight losses at 600°C reported in Table II. After functionalization with the RAFT agent, the SWCNT lost 12% of their weight. The SWCNT-RAFT was washed thoroughly with dichloromethane and dried before TGA analysis, but that does not prove that all organic material corresponding to the weight loss had been bound covalently to the SWCNT. Graft densities of the nitric acid treated SWCNT and the SWCNT-RAFT calculated from the TGA weight losses overestimate the number of functional groups because an unknown fraction of SWCNT carbon atoms may be lost along with the functional groups during heating. Assuming that the same amounts of SWCNT carbon atoms and RAFT functional groups were lost from the SWCNT-*g*-PMMA samples as from the SWCNT-RAFT sample, we calculate from curve c versus curves d, e, and f of Figure 1 that each SWCNT-*g*-PMMA sample was 5.9 wt % PMMA. This low PMMA content and the grafted PMMA molecular weights of 22,600–35,700 mean that less than 1% of the RAFT sites on the SWCNT actually produced PMMA. If the SWCNT were individual

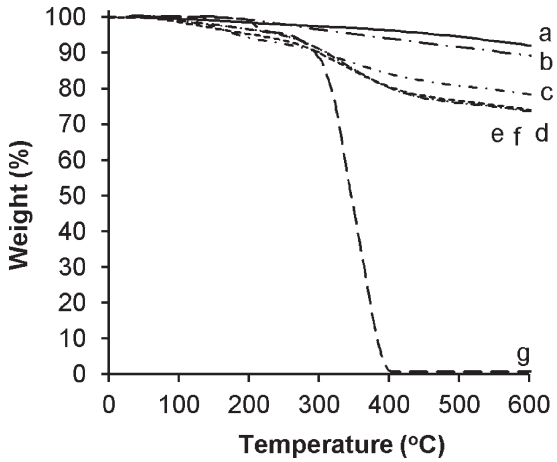

Figure 1. TGA under nitrogen heating at 10°C min^{-1} of (a) commercial SWCNT, (b) nitric acid treated SWCNT, (c) SWCNT-RAFT, (d) SWCNT-*g*-PMMA22600, (e) SWCNT-*g*-PMMA 26000, (f) SWCNT-*g*-PMMA35700, and (g) linear PMMA of $M_n = 44{,}100$ and $M_w/M_n = 1.2$ made by RAFT.

1.0-nm-diameter tubes, the graft density of PMMA would be 0.001 polymer chain per nm^2 of tube surface or approximately 1 chain for every 300 nm of nanotube length. TEM images show that the SWCNT existed as bundles, which have less external surface area than individual tubes, and therefore the graft density on bundles was significantly higher.

An important concern about the electrical properties of modified SWCNT is whether the functionalization of the tube ends and sidewalls affects the electronic structure of the tubes. The high electrical conductivity of SWCNT is due to the conjugated graphitic structure. Changes in electronic structure can be detected qualitatively from visible–NIR absorption and emission spectra, and alteration of the sidewalls can be detected from Raman spectra. The UV–vis–NIR absorption spectra of commercial SWCNT, nitric acid treated SWCNT, SWCNT-RAFT material, and SWCNT-*g*-PMMA in Figure 2 all show distinct first and second electronic transitions due to specific (*n*,*m*) types of tubes. This proves that the degree of functionalization is low, because high degrees of functionalization result in vis–NIR spectra that have no distinct peaks.[26] The NIR peaks cannot be assigned, however, because bundling of SWCNT perturbs the spectra.[27] Functionalization of SWCNT also can cause a large increase in the disorder/order (D/G) area ratio of peaks in resonance Raman spectra at about 1320 and 1580 cm^{-1}, respectively. The disorder peak is due to sp^3-hybridized carbon atoms in the tube sidewalls. The Raman spectra in Figure 3 all have very small disorder peaks, indicating that functionalization had little effect on the electronic structures of the tubes.

Table II. TGA of Functionalized SWCNT

Sample	% Weight loss[a]	Graft density[b]
SWCNT[c]	2.9	
SWCNT-RAFT	12.0	3.55
SWCNT-*g*-PMMA22600	17.9	0.03
SWCNT-*g*-PMMA26000	17.9	0.03
SWCNT-g-PMMA35700	17.9	0.02

[a] At 600°C relative to the starting SWCNT of curve b in Figure 1.
[b] Functional groups or PMMA chains/1000 SWCNT carbon atoms.
[c] Treated with nitric acid.

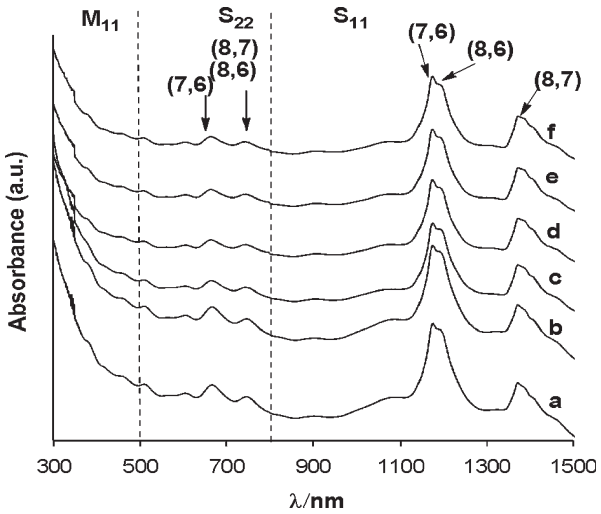

Figure 2. UV–vis–NIR spectra of (A) commercial SWCNT, (B) nitric acid treated SWCNT, (C) SWCNT-RAFT, (D) SWCNT-*g*-PMMA22600, (E) SWCNT-*g*-PMMA26000, and (F) SWCNT-*g*-PMMA35700.

Scanning transmission electron microscopy (STEM) images of the nitric acid treated SWCNT and the SWCNT-*g*-PMMA35700 are shown in Figure 4. (Images of the commercial SWCNT and SWCNT-*g*-PMMA26000 are in Supporting Information Figure S2). The lower resolution images in Figures 4(A) and 4(C) show long bundles having a wide range of diameters. The diameters of the bundles are not uniform, which means that the bundles consist of overlapping tubes of different lengths. The high resolution images of Figures 4(B) and 4(D) show individual parallel SWCNT in the bundles. The images of SWCNT-*g*-PMMA samples show intertwined bundles of SWCNT but no

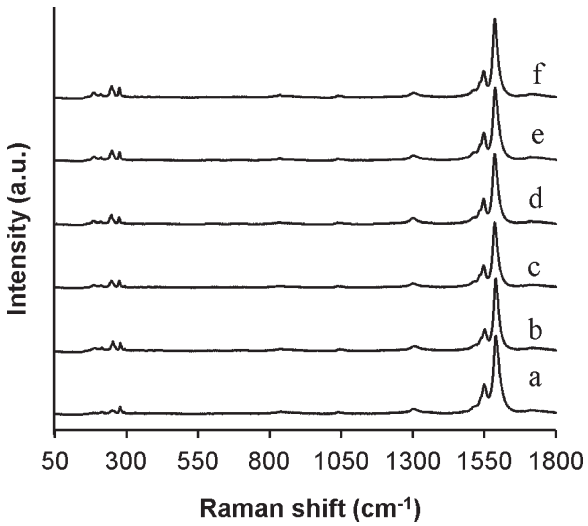

Figure 3. Resonance Raman spectra of (A) commercial SWCNT, (B) nitric acid treated SWCNT, (C) SWCNT-RAFT, (D) SWCNT-*g*-PMMA22600, (E) SWCNT-*g*-PMMA26000, and (F) SWCNT-*g*-PMMA35700.

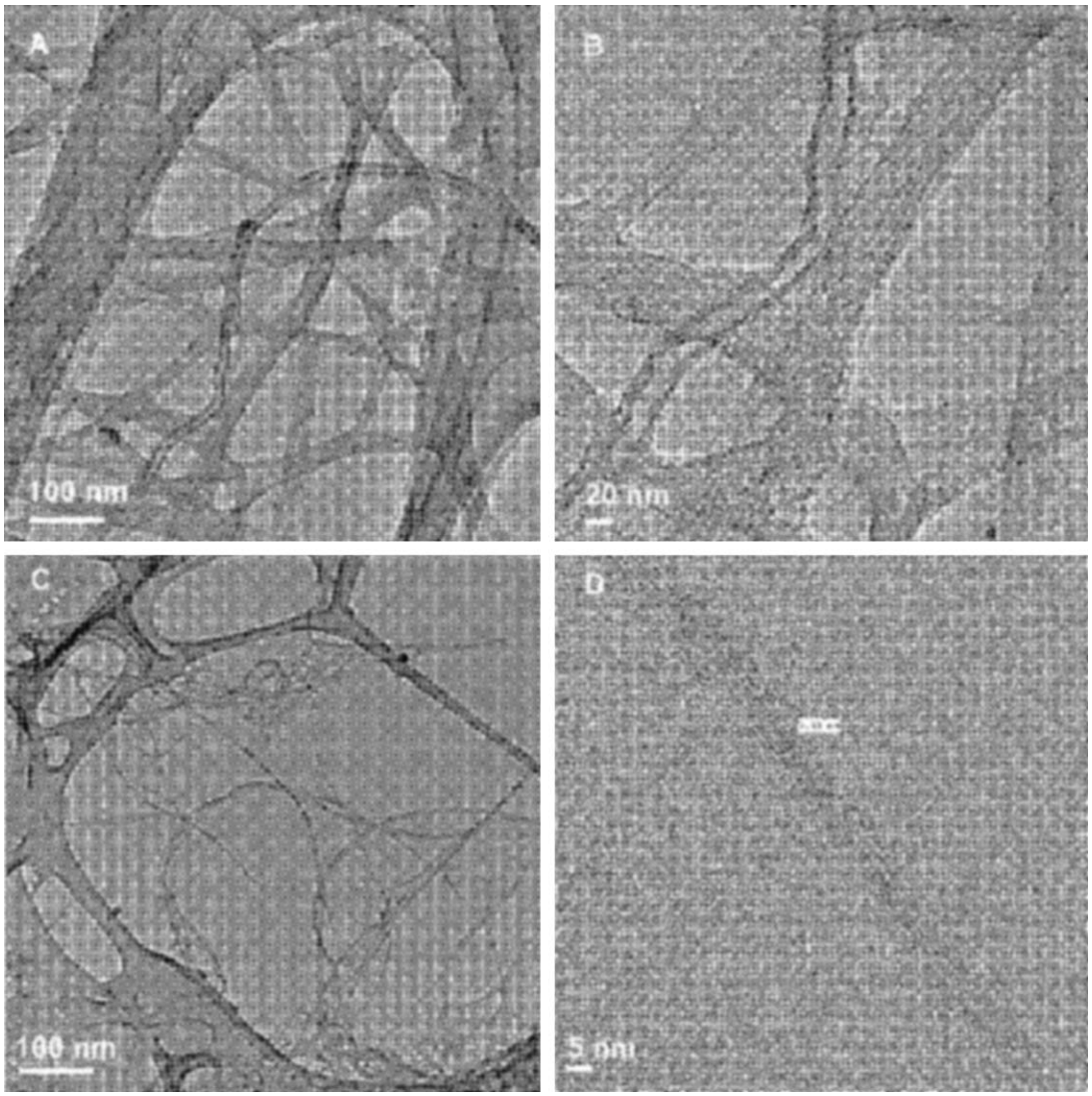

Figure 4. STEM images of nitric acid treated SWCNT (A, B) and SWCNT-*g*-PMMA35700 (C, D). In D the diameter at the marked point of a bundle is 7.31 nm.

PMMA is apparent, probably due to the low PMMA content (5.9 wt %) or to PMMA decomposition in the electron beam.

SWCNT-g-PMMA/PMMA Composites

We used RAFT polymerization to prepare three PMMA homopolymers as matrices for the SWCNT-*g*-PMMA/PMMA composites. Table III reports the polymerization conditions, molecular weights, and glass transition temperatures, which increased with increasing molecular weight as expected.

Table III. Synthesis Conditions and Molecular Weights of Matrix PMMA[a]

$[RAFT]_0$ ($M \times 10^2$)	M_n (g mol^{-1})	M_w/M_n	Yield (%)[b]	T_g (°C)
4.95	14,700	1.16	93	106
2.48	26,600	1.20	98	113
0.32	97,200	1.63	100	117

[a] MMA (6.55*M* in NMP), AIBN (0.0018*M*), and RAFT agent were heated for 6 h at 90°C.
[b] Measured gravimetrically.

The composites were prepared by mixing a dispersion of SWCNT-*g*-PMMA in NMP with a solution of matrix PMMA in THF and adding the mixed dispersion dropwise to water with stirring, a method known as coagulation/precipitation. Coagulation methods generally lead to good dispersion as judged by low percolation thresholds of electrical conductivity and increased storage modulus.[20,24,25,28] Three different matrix polymers were used with three different SWCNT-*g*-PMMA samples to obtain composites in which the matrix polymer had molecular weight less than, equal to, and greater than the molecular weight of the grafted PMMA. The contents of the three different sample types are listed in Table IV. Composites of each type containing 0.1–2.0 wt% of SWCNT were prepared. After drying, small amounts of the composite powders were analyzed by DSC. Larger amounts were heat pressed into thick films at 180°C for measurement of electrical conductivity and dynamic mechanical analysis.

Figures 5 and 6 show the results of DSC measurements of T_g and heat capacity change (ΔC_p) at T_g of the three types of

Table IV. Compositions of SWCNT-*g*-PMMA/PMMA Composites

M_n matrix[a]	M_n graft[b]
97,200	22,600
26,600	26,000
14,700	35,700

[a] From Table III
[b] From Table I

composites as a function SWCNT content. The T_g and ΔC_p of composites with $M_{graft} < M_{matrix}$ do not vary with amount of the SWCNT filler. The T_g of the composites with $M_{graft} = M_{matrix}$ increases slightly with increasing SWCNT content, and ΔC_p does not change significantly. The T_g of the composites with $M_{graft} > M_{matrix}$ increases up to 2.0% SWCNT while ΔC_p decreases from 0% to 0.5% SWCNT and then increases to 2.0% SWCNT.

Figure 7 shows graphs of two-probe electrical conductivities of the composite films. The films have percolation thresholds of 0.1–0.3% SWCNT for the composites with $M_{graft} = M_{matrix}$, 0.3–0.5% SWCNT for the composites with $M_{graft} > M_{matrix}$, and 0.5–1.0% for the composites with $M_{graft} < M_{matrix}$. The conductivities at 2.0% SWCNT were 10^{-9} to 10^{-11} S cm^{-1}, and decreased with increasing molecular weight of the matrix.

The composites with $M_{graft} = M_{matrix}$ and $M_{graft} < M_{matrix}$ were investigated by dynamic mechanical analysis (DMA). Composites with matrix $M_n = 14{,}700$ and $M_{graft} > M_{matrix}$ were too brittle for DMA measurements. Figures 8 and 9 show the temperature dependences of the storage modulus (E') and tan δ. E' of the composites increased little with increasing SWCNT content, and no there was no significant change in tan δ. T_g values measured from the DMA data were higher than T_g from DSC as expected because of the higher frequency of the DMA experiment. The rubbery plateau of both types of composites at >140°C broadened with increasing SWCNT which is indication

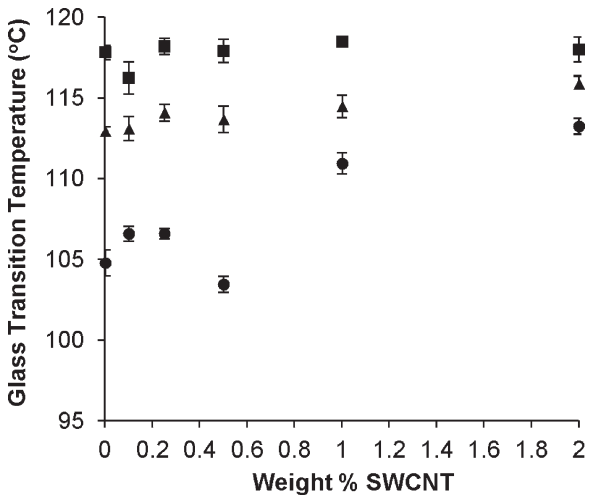

Figure 5. T_g of PMMA filled with SWCNT-*g*-PMMA. (■) Matrix $M_n = 97{,}200$ and graft $M_n = 22{,}600$. (▲) Matrix $M_n = 26{,}600$ and graft $M_n = 26{,}000$. (•) Matrix $M_n = 14{,}700$ and graft $M_n = 35{,}700$. The error bars are standard deviations of six measurements.

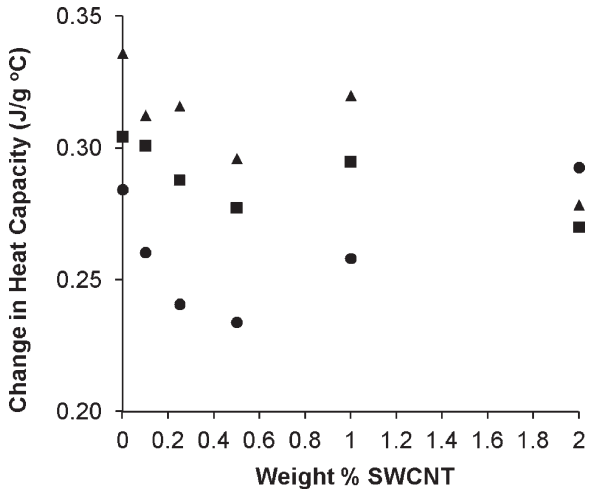

Figure 6. ΔC_p at T_g of PMMA filled with SWCNT-*g*-PMMA. (■) Matrix $M_n = 97{,}200$ and graft $M_n = 22{,}600$. (▲) Matrix $M_n = 26{,}600$ and graft $M_n = 26{,}000$. (•) Matrix $M_n = 14{,}700$ and graft $M_n = 35{,}700$. Standard deviations of six measurements of each sample ranged from ± 0.015 to ± 0.03 J g^{-1}°C^{-1}.

of the beginnings of network formation as described elsewhere.[29] In other words, the dispersed SWCNT-*g*-PMMA makes the composites more rubbery at $T > T_g$ and correspond to an increase storage of or steady-shear viscosity common in nanotube-filled systems.

DISCUSSION

Grafting of PMMA from SWCNT

Polymers can be "grafted to" or "grafted from" surfaces such as silicon wafers, silica and other metal oxide particles, and carbon nanotubes. Generally grafting from provides a higher density of chains because the initiator or chain transfer functional groups

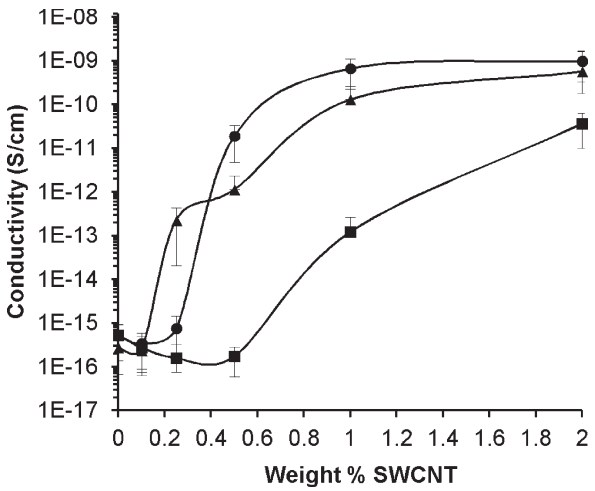

Figure 7. Electrical conductivity of PMMA filled with SWCNT-*g*-PMMA. (■) Matrix $M_n = 97{,}200$ and graft $M_n = 22{,}600$. (▲) Matrix $M_n = 26{,}600$ and graft $M_n = 26{,}000$. (•) Matrix $M_n = 14{,}700$ and graft $M_n = 35{,}700$. Data points are the average of data recorded at 30 V and at 100 V. Error bars represent the standard deviation of measurements on the same sample made multiple times; the error bars are asymmetric because averages were calculated on the values, not the logarithm of the values.

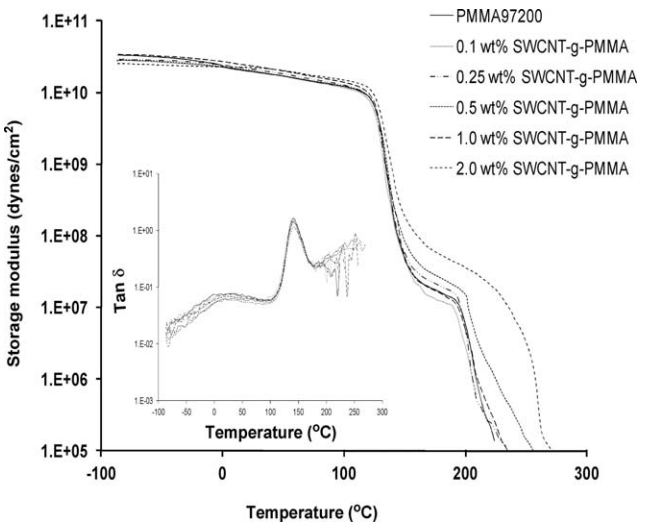

Figure 8. Storage modulus and tan δ of SWCNT-*g*-PMMA22600/PMMA26000 measured by DMA with temperature sweep at 1 Hz and 0.05% strain.

can be created at high surface density, whereas grafting to is sterically hindered by previously grafted polymer chains. Grafting from can be performed by atom transfer radical polymerization (ATRP),[22,30–32] by reversible addition fragmentation transfer polymerization (RAFT), in which a dithioester[33] or trithiocarbonate[34] chain transfer group is prepared on the surface, and by polymerization from a surface-bound initiator.[35] Grafting from by radical chain polymerization from SWCNT could be complicated by reaction of carbon radicals with the sidewalls of the tubes, which have strained carbon–carbon double bonds. Although SWCNT do not react as fast as C_{60} with carbon radicals,[36] nitroxide-terminated polystyrene grafts readily to SWCNT.[20] Most literature reports of RAFT polymerization from carbon nanotubes employed multi-walled carbon nanotubes (MWCNT) which react slower than SWCNT with carbon

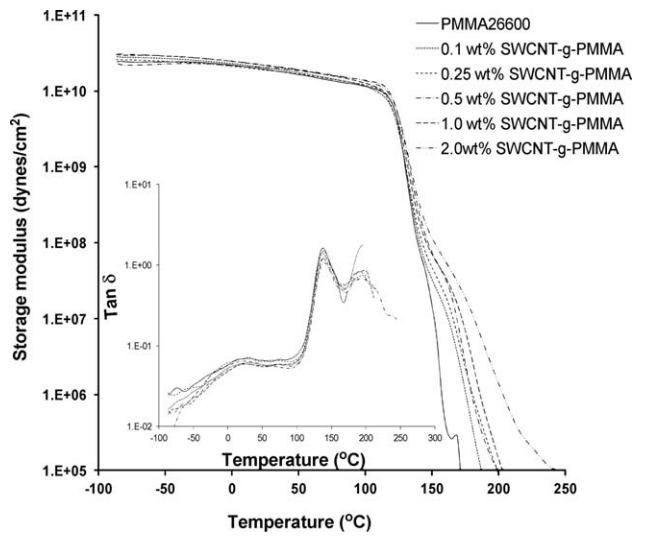

Figure 9. Storage modulus and tan δ of SWCNT-*g*-PMMA22600/PMMA97200 measured by DMA with temperature sweep at 1 Hz and 0.05% strain.

radicals because the outer tube of a MWCNT has a greater diameter and is less strained than a SWCNT.

Because RAFT also produces ungrafted free polymer, separation of free polymer from surface-bound polymer is necessary for investigation of how polymer-grafted particles interact with a matrix of controlled molecular weight in a composite. Such separations can be difficult. Also it is difficult to prove that all of the free polymer has been removed from a sample of polymer-grafted particles.[37] We chose RAFT for this research following the examples of Benicewicz and coworkers for grafting polystyrene and poly(meth)acrylates from silica nanoparticles.[11,38–40] Evidence that RAFT polymerization grafted PMMA from SWCNT in this work is as follows. (1) After functionalization of the SWCNT with the RAFT agent as in Scheme 1, TGA showed 12 wt % of degradable material, NMR spectra showed the desired RAFT trithioester, and elemental analysis found 0.85% S. All of these observations support extensive functionalization with the RAFT agent. (2) Both PMMA bound to SWCNT and ungrafted PMMA were isolated after polymerization. The ungrafted PMMA and the PMMA that was isolated by cleavage of PMMA from the SWCNT had different molecular weights and molecular weight distributions. (3) After separation of ungrafted PMMA the NMR spectrum of the SWCNT-*g*-PMMA showed both bound PMMA and residual bound RAFT agent. (4) Varied relative molecular weights of the grafted PMMA and the matrix PMMA of the composites gave varied T_g of the composites, which is consistent with theory for wetting or dewetting the SWCNT by grafted PMMA. The autophobic dewetting evidence is discussed below.

SWCNT-g-PMMA/PMMA Composites

Literature reports of the effect of SWCNT and of silica nanoparticles on T_g of PMMA in composites vary widely. PMMA grafted to silica by RAFT gave no change in T_g of composites up to 15 wt % silica.[41] Up to 20 wt% silica changed $T_g \leq 1°C$ in bulk samples,[41,42] and 0.5% silica increased T_g by 6°C in thin films.[43] In situ polymerization of PMMA in the presence of SWCNT to prepare SWCNT-*g*-PMMA followed by dispersion into matrix PMMA gave no change of T_g in one report[44] and a 6°C increase in T_g at 2% SWCNT in another report.[35] Dispersing up to 2 wt % of unmodified SWCNT into PMMA changed T_g by $\leq 2°C$ in one report[24] and increased T_g by up to 18°C in other reports.[45–47] These variations in results are probably due to the widely different processing methods. Comparisons of composites prepared by one method in one laboratory, on the other hand, should be valid. Our SWCNT-*g*-PMMA caused only small changes in T_g of the matrix PMMA but differed as a function of the relative molecular weights of the grafted and matrix PMMA.

A matrix polymer will mix with (wet) a chemically identical polymer grafted from a surface only if the entropy lost by matrix chains penetrating the grafted chains is less than the entropy gained by mixing.[9–19] The condition of net decrease of entropy is known as autophobic dewetting. Chains attached to a planar surface at low graft density have a mushroom shape due to a random coil with one anchored end. At high graft density packing forces the chains to extend farther from the surface,

and the grafted chains are constrained so that extension occurs only in one dimension. Although small molecules penetrate the grafted chains at high density, the positive entropy of mixing of chemically identical long chain matrix polymers is too small to compensate for the negative entropy change of matrix chains confined by the grafted chains on the surface. Numerous experiments support autophobic dewetting. At low graft density, it is easier for solvents and polymers of all sizes to mix with grafted chains, which has been shown by AFM observation of increasing aggregation with increasing density of grafting of PS to 14 nm diameter silica spheres.[14] The density of grafted chains decreases as the radius of gyration (R_g) of the grafted chains increases with respect to the particle radius and increases with decreasing sphere radius,[12] which has been verified by increased dispersion into matrix poly(dimethylsiloxane) (PDMS) of spheres of silica-*g*-PDMS of decreasing radius of 592, 100, and 16 nm.[48] In other words, the volume available for extension becomes larger as one moves away from the surface. Silica spheres of 14-nm-diameter grafted at a density of 0.27 chains nm^{-2} with PS of *DP* 1050 are wetted by PS matrices of $DP \leq 620$, as T_g increases with added filler, and not wetted by PS of $DP = 860$, as T_g decreases with added filler.[11] Similar results were reported for PS composites containing TiO_2-*g*-PS particles.[49] Experimentally wetting/autophobic dewetting of polymer-grafted silica particles in a polymer matrix also has been observed by rheology of particle-polymer mixtures,[15,48,50] SAXS,[15] neutron scattering,[13,50] X-ray photon correlation spectroscopy[41] AFM of film and bulk composite surfaces,[13,14] and TEM.[19,41,51] Note that aggregation by polymer bridging between nanospheres provides mechanical reinforcement of the composite; that is, poorer dispersion results in greater mechanical strength.[41,50]

Polymers grafted from bundles of SWCNT extend in two dimensions. The chains should be less densely packed than chains grafted from a planar surface and more densely packed than chains grafted from the surface of a nanosphere of the same diameter. Composto[52] reported PS grafted to 12 nm × 42 nm gold nanorods at surface densities of 0.15–0.53 chains nm^{-2}. The nanorods dispersed in a PS matrix when $M_{graft} > M_{matrix}$ and aggregated when $M_{graft} < M_{matrix}$. Dispersions of Au-*g*-PEG [PEG = poly(ethylene glycol) of $M_w = 5000$] in PMMA and in PEO [poly(ethylene oxide)] of higher M_w were made; the PEG brushes dispersed into PMMA due to favorable enthalpic interaction and not into PEO due to net decrease of entropy.[53] We do not know the diameters of our bundles of SWCNT-*g*-PMMA and therefore do not know the surface density of grafted PMMA chains. Six weight percent of grafted PMMA on the SWCNT corresponds to a surface chain graft density of 0.001 nm^{-2} if the SWCNT were all individual tubes and a surface graft density of 0.004 nm^{-2} if the SWCNT were all 5-nm-diameter bundles of nanotubes (assuming 1-nm-diameter individual tubes, hexagonal packing of parallel cylindrical tubes, and PMMA of $M_n = 26{,}000$).

Despite the low surface graft density of PMMA on SWCNT, T_g of the composites still varied with relative *DP* of the grafted and the matrix polymers consistent with autophobic dewetting: When $M_{graft} > M_{matrix}$, T_g increased with increasing weight percent of SWCNT and when $M_{graft} \leq M_{matrix}$, T_g did not change with increasing amount of nanotubes. The former is consistent with wetting and the latter is consistent with dewetting. The results suggest that the SWCNT-*g*-PMMA in the composites is less aggregated when $M_{graft} > M_{matrix}$, and therefore these composites should have a lower percolation threshold of electrical conductivity, which indeed is the result in Figure 7. We conclude that the SWCNT-*g*-PMMA/PMMA composites exhibit autophobic dewetting when $M_{graft} \leq M_{matrix}$ even with a low surface graft density. Because of autophobic dewetting, the percolation threshold of electrical conductivity is expected to be higher for SWCNT-*g*-PMMA/PMMA than for unfunctionalized SWCNT/PMMA composites, contrary to the simple "like dissolves like" prediction that the SWCNT-*g*-PMMA should disperse better than unfunctionalized SWCNT. Although we have not investigated dispersions of unfunctionalized SWCNT in PMMA, dispersions of SWCNT-*g*-PS in PS, using the same method of composite preparation as in this paper, had a higher threshold of electrical conductivity than dispersions of unfunctionalized SWCNT in PS, which is consistent with autophobic dewetting.[20]

The data in Figure 7 show that all three of the composites have relatively low electrical conductivity at SWCNT contents above the percolation threshold, which may be due to the grafted PMMA acting as an insulating barrier to electron hopping between nanotube bundles, as we suggested for SWCNT-*g*-PS/PS composites.[20] Also significant is the higher percolation threshold (>0.5 wt % nanotubes) of the composite in which the lower molecular weight matrix wets the higher molecular weight graft. The higher percolation threshold with higher *DP* of grafted PMMA also might be due to effective PMMA insulation between nanotube bundles. Percolation thresholds in the same range as in Figure 7 have been noted before for SWCNT/PMMA composites that were prepared by a coagulation method.[28,54] Lacking grafted PMMA, the conductivities of SWCNT/PMMA composites containing 0.5 wt % SWCNT increased with increasing UV–vis–NIR absorbance of the samples, which corresponds to increasing dispersion of the SWCNT into smaller bundles.[28]

PMMA also has been grafted to SWCNT using a surface bound azo initiator to give SWCNT-*g*-PMMA containing 82% PMMA by weight after extraction of ungrafted PMMA, which is much higher than the PMMA content in our materials.[35] A PMMA composite of this material containing 2.17 wt % SWCNT had T_g 6°C higher than both pure PMMA and a blend of SWCNT and PMMA. Both the grafted polymer and the matrix polymer had broad molecular weight distributions. The similarity of both the T_g and the electrical conductivity changes in our composites compared with others having much higher PMMA content, might be explained by much larger diameter average bundles of SWCNT than we calculated for bundles of 5 nm diameter, and therefore higher graft densities than is indicated by the TEM images of Figure 4, more like the graft densities of other SWCNT-*g*-PMMA materials.[28,35]

CONCLUSIONS

SWCNT having a low concentration of surface COOH groups were functionalized with an initiator of RAFT polymerization, and PMMA was grafted to give SWCNT-*g*-PMMA containing

6 wt % of PMMA. SWCNT-*g*-PMMA having grafted M_n = 22,600–35,700 were dispersed into matrices of low polydispersity PMMA having M_n = 14,700–97,200. The surface densities of grafted PMMA chains could not be determined because the diameters of the bundles of SWCNG-*g*-PMMA in the composites resisted imaging by STEM. From measurements of the composites as a function of SWCNT content, matrix PMMA of M_n greater than M_n of grafted PMMA had little effect on the properties whereas matrix PMMA of M_n less than M_n of grafted PMMA increased T_g and decreased the percolation threshold of electrical conductivity of the composites. The results are consistent with wetting of SWCNT-*g*-PMMA by the lower but not the higher M_n matrix.

ACKNOWLEDGMENTS

BPG acknowledges the financial support given by the Department of Energy (Grant ER64239 0012293). WTF and AP thank the Oklahoma State Regents for Higher Education for partial support of this research, Prof. Daniel E. Resasco and Veronica M. Iruzun of the University of Oklahoma for the Raman spectra and Prof. Jan Hanan for use of the hydraulic press.

REFERENCES

1. Grady, B. P. *Carbon Nanotube-Polymer Composites: Manufacture, Properties, and Applications*. Wiley : New York, **2011**.
2. Coleman, J. N.; Khan, U.; Blau, W. J.; Gun'ko, Y. K. *Carbon* **2006**, *44*, 1624.
3. Winey, K. I.; Vaia, R. A. *MRS Bull.* **2007**, *32*, 314.
4. Krishnamoorti, R.; Vaia, R. A. *J. Polym. Sci. Part B: Polym. Phys.* **2007**, *45*, 3252.
5. Shull, K. R. *J. Chem. Phys.* **1991**, *94*, 5723.
6. Clarke, C. J.; Jones, R. A. L.; Edwards, J. L.; Shull, K. R.; Penfold, J. *Macromolecules* **1995**, *28*, 2042.
7. Laub, C. F.; Koberstein, J. T. *Macromolecules* **1994**, *27*, 5016.
8. Liu, Y.; Rafailovich, M. H.; Sokolov, J.; Schwarz, S. A.; Zhong, X.; Eisenberg, A.; Kramer, E. J.; Sauer, B. B.; Satija, S. *Phys. Rev. Lett.* **1994**, *73*, 440.
9. Ferreira, P. G.; Ajdari, A.; Leibler, L. *Macromolecules* **1998**, *31*, 3994.
10. Oslanec, R.; Costa, A. C.; Composto, R. J.; Vlcek, P. *Macromolecules* **2000**, *33*, 5505.
11. Bansal, A.; Yang, H.; Li, C.; Benicewicz, B. C.; Kumar, S. K.; Schadler, L. S. *J. Polym. Sci. Part B: Polym. Phys.* **2006**, *44*, 2944.
12. Harton, S. E.; Kumar, S. K. *J. Polym. Sci. Part B: Polym. Phys.* **2008**, *46*, 351.
13. Kalb, J.; Dukes, D.; Kumar, S. K.; Hoy, R. S.; Grest, G. S. *Soft Matter* **2011**, *7*, 1418.
14. Maillard, D.; Kumar, S. K.; Rungta, A.; Benicewicz, B. C.; Prud'homme, R. E. *Nano Lett.* **2011**, *11*, 4569.
15. Lan, Q.; Francis, L. F.; Bates, F. S. *J. Polym. Sci. Part B: Polym. Phys.* **2007**, *45*, 2284.
16. Xu, J.; Qiu, F.; Zhang, H.; Yang, Y. *J. Polym. Sci. Part B: Polym. Phys.* **2006**, *44*, 2811.
17. Trombly, D. M.; Ganesan, V. *J. Chem. Phys.* **2010**, 133.
18. Green, P. F. *Soft Matter* **2011**, *7*, 7914.
19. Green, P. F.; Oh, H.; Akcora, P.; Kumar, S. K. In *Dynamics of Soft Matter: Neutron Applications, Neutron Scattering Applications and Techniques*, Sakai, V. G., Alba-Simionesco, C., Chen, S., Eds.; Springer : Philadelphia, **2012**; pp 349–366.
20. Paul, A.; Grady, B. P.; Ford, W. T. *Polym. Int.* **2012**.
21. Tchoul, M. N.; Ford, W. T.; Lolli, G.; Resasco, D. E.; Arepalli, S. *Chem. Mater.* **2007**, *19*, 5765.
22. Qin, S.; Qin, D.; Ford, W. T.; Resasco, D. E.; Herrera, J. E. *J. Am. Chem. Soc.* **2004**, *126*, 170.
23. Magenau, A. J. D.; Martinez-Castro, N.; Storey, R. F. *Macromolecules* **2009**, *42*, 2353.
24. Du, F.; Scogna, R. C.; Zhou, W.; Brand, S.; Fischer, J. E.; Winey, K. I. *Macromolecules* **2004**, *37*, 9048.
25. Tchoul, M. N.; Ford, W. T.; Ha, M. L. P.; Chavez-Sumarriva, I.; Grady, B. P.; Lolli, G.; Resasco, D. E.; Arepalli, S. *Chem. Mater.* **2008**, *20*, 3120.
26. Dyke, C. A.; Tour, J. M. *Nano Lett.* **2003**, *3*, 1215.
27. Weisman, R. B.; Bachilo, S. M. *Nano Letters* **2003**, *3*, 1235.
28. Kashiwagi, T.; Fagan, J.; Douglas, J. F.; Yamamoto, K.; Heckert, A. N.; Leigh, S. D.; Obrzut, J.; Du, F.; Lin-Gibson, S.; Mu, M.; Winey, K. I.; Haggenmueller, R. *Polymer* **2007**, *48*, 4855.
29. Ha, M.; Grady, B.; Lolli, G.; Resasco, D.; Ford, W. *Macromol. Chem. Phys* **2007**, *208*, 446.
30. Yao, Z.; Braidy, N.; Botton, G. A.; Adronov, A. *J. Am. Chem. Soc.* **2003**, *125*, 16015.
31. Kong, H.; Gao, C.; Yan, D. *Macromolecules* **2004**, *37*, 4022.
32. Homenick, C. M.; Lawson, G.; Adronov, A. *Polym. Rev.* **2007**, *47*, 265.
33. Hong, C.-Y.; You, Y.-Z.; Pan, C.-Y. *J. Polym. Sci., Part A: Polym. Chem.* **2006**, *44*, 2419.
34. You, Y.-Z.; Hong, C.-Y.; Pan, C.-Y. *Nanotechnology* **2006**, *17*, 2350.
35. Cui, L.; Tarte, N. H.; Woo, S. I. *J. Appl. Polym. Sci.* **2011**, *119*, 452.
36. Guldi, D. M.; Ford, W. T.; Nishioka, T. *Proc. Electrochem. Soc.* **1999**, *99-12*, 315.
37. Tchoul, M. N.; Dalton, M.; Tan, L.-S.; Dong, H.; Hui, C. M.; Matyjaszewski, K.; Vaia, R. A. *Polymer* **2012**, *53*, 79.
38. Bansal, A.; Yang, H.; Li, C.; Cho, K. J.; Benicewicz, B. C.; Kumar, S. K.; Schadler, L. S. *Nature Mater.* **2005**, *4*, 693.
39. Li, C.; Benicewicz, B. C. *Macromolecules* **2005**, *38*, 5929.
40. Li, C.; Han, J.; Ryu, C. Y.; Benicewicz, B. C. *Macromolecules* **2006**, *39*, 3175.
41. Akcora, P.; Kumar, S. K.; Sakai, V. G.; Li, Y.; Benicewicz, B. C.; Schadler, L. S. *Macromolecules* **2010**, *43*, 8275.
42. Moll, J.; Kumar, S. K. *Macromolecules* **2012**, *45*, 1131.
43. Rittigstein, P.; Torkelson, J. M. *J. Polym. Sci. Part B: Polym. Phys.* **2006**, *44*, 2935.
44. Vigolo, B.; Vincent, B.; Eschbach, J.; Bourson, P.; Mareche, J.-F.; McRae, E.; Mueller, A.; Soldatov, A.; Hiver, J.-M.; Dahoun, A.; Rouxel, D. *J. Phys. Chem. C* **2009**, *113*, 17648.

45. Muisener, P. A. O. R.; Clayton, L.; D'Angelo, J.; Harmon, J. P.; Sikder, A. K.; Kumar, A.; Cassell, A. M.; Meyyappan, M. *J. Mater. Res.* **2002**, *17*, 2507.

46. Kumar, S.; Rath, T.; Khatua, B. B.; Dhibar, A. K.; Das, C. K. *J. Nanosci. Nanotech.* **2009**, *9*, 4644.

47. Pradhan, N. R.; Iannoachione, G. S. *J. Phys. D Appl. Phys.* **2010**, *43*, 305403.

48. McEwan, M.; Green, D. *Soft Matter* **2009**, *5*, 1705.

49. Tchoul, M. N.; Fillery, S. P.; Koerner, H.; Drummy, L. F.; Oyerokun, F. T.; Mirau, P. A.; Durstock, M. F.; Vaia, R. A. *Chem. Mater.* **2010**, *22*, 1749.

50. Dukes, D.; Li, Y.; Lewis, S.; Benicewicz, B. C.; Schadler, L. S.; Kumar, S. K. *Macromolecules* **2010**, *43*, 1564.

51. Akcora, P.; Kumar, S. K.; Moll, J.; Lewis, S.; Schadler, L. S.; Li, Y.; Benicewicz, B. C.; Sandy, A.; Narayanan, S.; Ilavsky, J.; Thiyagarajan, P.; Colby, R. H.; Douglas, J. F. *Macromolecules* **2010**, *43*, 1003.

52. Chung, H.-J.; Kim, J.; Ohno, K.; Composto, R. *J. ACS Macro Lett.* **2012**, *1*, 252.

53. Hore, M. J. A.; Composto, R. *J. ACS Nano* **2010**, *4*, 6941.

54. Du, F.; Fischer, J. E.; Winey, K. I. *J. Polym. Sci. Part B: Polym. Phys.* **2003**, *41*, 3333.